



ELSEVIER

Physica C 357–360 (2001) 489–493

PHYSICA C

www.elsevier.com/locate/physc

Perfect fits of J_c – B dependencies in NEG-123 bulk samples with 30% Gd-211 fine particles

M. Jirsa^{a,b,*}, M. Muralidhar^b, M. Murakami^b^a Czech Academy of Sciences, Institute of Physics ASCR, Na Slovance 2, CZ-182-21 Praha 8, Czech Republic^b Superconductivity Research Laboratory, ISTEC, 16-25 Shibaura 1-chome, Minato-ku, Tokyo 105-0023, Japan

Received 16 October 2000; accepted 25 November 2000

Abstract

Magnetization hysteresis loops (MHL) were measured on two NEG-123 bulk samples with addition of 30% Gd-211 fine (sub-micron) particles in the temperature range 65–88 K. These two samples possessed significantly different second-to-central peak heights ratios. Both sets of the J_c – B curves could be, however, fitted with a high precision by the same combined analytical function $J_c(B) = J_{cp} \exp(-\alpha B/B_p) + J_{sp} b_p \exp[(1 - (B/B_p)^n)/n]$ in all investigated temperatures. The pinning regimes governing formation of the central and second peak could be separated in this way. As far as the central peak contribution to the MHL becomes usually negligible at around B_p , the shape of $J_c(B)$ above B_p is governed by only a high-field pinning mechanism. The central peak extends to this field region only at temperatures very close to T_c . Good scaling of the pinning force density with temperature gives a further support to the above conclusions. © 2001 Elsevier Science B.V. All rights reserved.

PACS: 74.60.Ec; 74.60.Ge; 74.60.Jg

Keywords: Vortex physics; Critical currents; Scaling; Melt-textured materials; (Nd,Eu,Gd)Ba₂Cu₃O₇

1. Introduction

Many bulk RE-123 samples show scaling properties of $J_c(B)$ and $F_p(B) = BJ_c(B)$ dependencies in a more or less limited temperature range and it is believed that this property reflects vortex pinning in the material and can therefore serve for classification of pinning strength. Due to the lack of a satisfactory theory, classical models have been frequently used to fit experimental data, neglecting effects of huge relaxation, strong anisotropy, and

other attributes of high- T_c materials. Though such a fit can be successful [1], the resulting values of free parameters are usually out of the range predicted by original models [2]. Moreover, the central peak on the MHLs evidently does not scale in the same manner as the second peak, giving thus evidence of a different pinning mechanism involved. The exact theoretical description of this peak is also still missing.

In this paper we present experimental data of two samples cut from the same pellet and processed together in the same manner. In spite of that, they exhibited quite different second peak appearance. We employed this situation as a test of our recent phenomenological model based on

* Corresponding author. Tel.: +420-2-6605-2718; fax: +420-2-821227.

E-mail address: jirsa@fzu.cz (M. Jirsa).

the assumption of a thermally activated pinning process and a logarithmic pinning potential.

2. Experimental

The investigated samples were oxygen-deficient-melt-growth (OCMG) processed samples of $(\text{Nd}_{0.33}\text{Eu}_{0.33}\text{Gd}_{0.33})\text{Ba}_2\text{Cu}_3\text{O}_{7-\delta}$ (NEG-123) doped by 30 mol% of fine (sub-micron) Gd-211 particles. These were refined by addition of 0.5 mol% of Pt and 1 mol% CeO_2 . The exact technological treatment was described in Ref. [3]. The samples were cut from the place approximately 6 mm apart of the center of the pellet 1 cm high and 18 mm in diameter, one sample from the middle of the pellet (sample LLM), the other from the bottom (sample LLB). The samples had dimensions of $1.5 \times 1.5 \times 0.5 \text{ mm}^3$. Both samples were annealed together in 1 bar O_2 atmosphere at 600–300°C for 240 h. The typical second phase particles (SPP) distribution is shown in Fig. 1. The average size of the particles is shown in Fig. 1. The average size of the particles was less than 1 μm , the smallest ones were of about 0.1 μm in diameter. Surprisingly, the concentration of the SPP was in both samples nearly equal. After polishing the samples, magnetization hysteresis curves (MHL) were measured by means of a standard Quantum Design SQUID magnetometer in temperature range 65–88 K and magnetic fields to 7 T, with the field oriented along the c -axis. Critical current density was calculated from the magnetic hysteresis using the modified Bean model [4], $J_c = \Delta M / \Omega$, with $\Omega = \frac{1}{2}a^2d(b - a/3)$. Here ΔM is the difference of magnetic moments on the upper and lower MHL branch, a , b are lateral dimensions of the sample and d is its thickness.

3. Experimental results

The hysteresis loops measured in the temperature range 60–88 K and fields up to 7 T are presented in Fig. 2 for the sample LLM and in Fig. 3 for the sample LLB. The appearance of the MHL is in both samples quite different. Though the heights of the central peaks and irreversibility fields are in both samples similar, the second peak

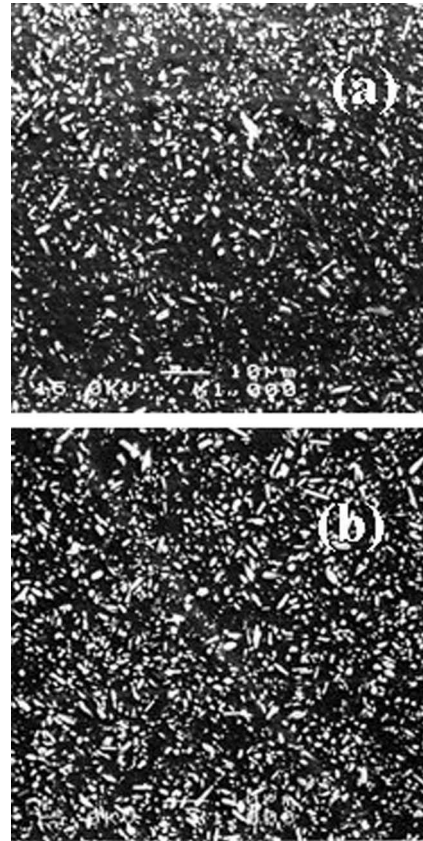


Fig. 1. SEM images of the secondary phase particles distribution in NEG-123 samples doped by 30 mol% of Gd-211, (a) sample LLM, (b) sample LLB.

in the sample LLB is strongly suppressed. This was caused by diffusion of ZrO_2 into the pellet from a support rod used during the melt-texturing process. As the melting temperature of Gd-211 particles is higher than that of the NEG-123 matrix, the SPPs were not practically affected by the reaction with ZrO_2 . Although this sample was of worse quality, it exhibited the same T_c onset as the other one, namely 93.6 K. In the sample LLM the superconducting transition observed on the dc susceptibility was complete within 1 K, in the sample LLB 80% of the transition was the same but in the rest a tail appeared extending up to 85.5 K. The different characteristics of these samples prepared under same conditions, of the same material, and annealed simultaneously enable to study pinning

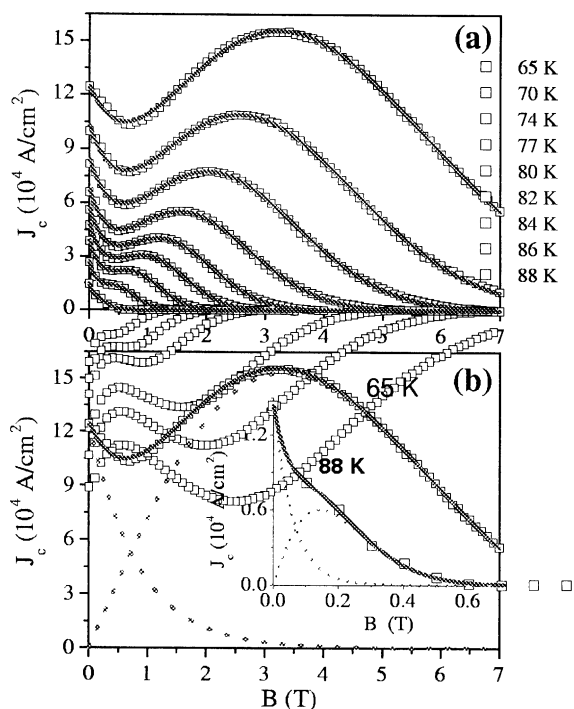


Fig. 2. $J_c(B)$ dependencies deduced from magnetization measurements by SQUID on the sample LLM (symbols). The full lines are fits by means of Eq. (1). Dotted lines indicate individual contributions from the two terms in Eq. (1), of the central and second peak.

mechanisms in more detail. As the SPP concentration was nearly the same, we conclude that these particles do not contribute to the formation of the second peak directly. On the other hand, the same morphology of SPPs in both samples is in accord with the same heights of the central peaks [5].

The secondary phase particles were also suggested as a source of a “background” pinning [6,7]. To test this hypothesis, we decomposed the experimental curves indicated by symbols in Figs. 2 and 3 into two separate contributions using a combined fitting function

$$J_c(B) = J_{p1} \exp(-wb_p) + J_{p2} b_p \exp[(1 - b_p^n)/n], \quad (1)$$

where J_{p1} and J_{p2} are heights of the central and second peak, respectively, w and n are the exponential decay rates, and $b_p = B/B_p$, B_p being position of the second peak. J_{p1} was fixed at the experimental value; J_{p2} was let as a free parameter,

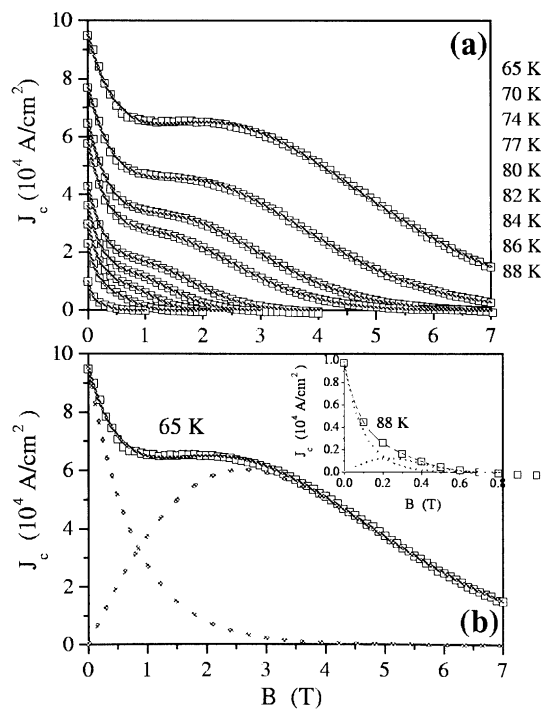


Fig. 3. The same as in Fig. 2 for the sample LLB.

together with B_p , w , and n . This choice introduced the necessary freedom for the second peak (second term in Eq. (1)). The second term follows from the model of thermally activated flux creep with a logarithmic pinning potential [1,8–11], the first term was found empirically by subtracting the second peak term from experimental data [10].

The fits (full lines in the figures) were successful in both samples with so different shapes of MHL. In the sample LLB the second peak was well developed in most of the investigated temperatures and it occurred that the height and position of this peak on the *experimental* curve nearly coincided with that of the separated *theoretical* peak. In other words, the central peak contribution decayed so fast that it practically disappeared below B_p . This means that the upper slope of the second peak on the experimental $J_c(B)$ curve was governed exclusively by the pinning mechanism responsible for the second peak (e.g. point-like pinning disorder) and did not mix with any “background” contribution. In the studied sample the central peak extended to the fields above B_p

only in a close vicinity of T_c where the second peak was already very weak. The fits in this sample were of nearly same quality with J_{p2} and B_p fixed in their experimental values, leaving thus only two free parameters, w and n .

In the sample LLB the second peak was not well recognizable directly from the experimental data but the decomposition into separate contributions of the central and second peak showed that the latter one is weak but present up to highest temperatures (see inset in Fig. 3(b)). Especially in this sample the central peak became dominant at temperatures close to T_c . We note that this feature differs from the behavior of RE-123 single crystals where with increasing temperature the central peak usually decreases faster than the second peak. This difference evidently originates in the absence of the rather large secondary phase particles in single crystals. The pinning on these particles was shown to enhance the central peak. It is obviously less sensitive to temperature rise [3,12]. This indicates that the pinning efficiency of SPPs is larger than that of point-like defects, most probably due to a larger effective pinning volume. On the other hand, the efficiency of SPP is limited to low field region and rapidly decreases with increasing vortex concentration. Only at high temperatures, where the pinning landscape of the point-like disorder becomes washed out, the pinning on SPPs starts to play a significant role also in fields close to B_{irr} . In this case, however, B_{irr} is low, which in turn suites to the pinning mechanism on the SPP structure. From plots of temperature dependencies of the fitting parameters we learned that the position of the second peak increased with decreasing temperature nearly linearly but the irreversibility field increased much faster. In both samples there was only a close temperature range where the $J_c(B)$ curves scaled with temperature (65–77 K), which was deduced from a temperature-independent value of n [1,10,11].

Pinning force density $F(B) = BJ_c(B)$ curves exhibited much better scaling than $J_c(B)$, which extended over the whole investigated temperature range, especially in the sample LLM. From theoretical point of view there is no reason for a different behavior of $F(B)$ and $J_c(B)$ except the peak on an $F(B)$ dependence lies at significantly higher

fields than that on the corresponding $J_c(B)$. We conclude that the pinning process at higher fields, around and above the peak on the $F(B)$ curve, is better defined and more uniform than around B_p . Moreover, the central peak that scales in a different way [1,11] is in the $F(B)$ dependence effectively suppressed. The $F(B)$ curve is therefore very suitable for the performance classification of novel superconducting materials.

4. Conclusions

The analysis of experimental data of two melt-textured samples showed that the experimental curved can be successfully modeled by two independent contributions related to the central and second peak of MHL. The former one decays exponentially with increasing field and does not usually extend behind the second peak maximum. The temperature dependencies of both terms indicate that the flux pinning by secondary phase particles is more efficient than that of a point-like disorder but is limited to low fields only, enhancing first of all the central peak. No “background” contribution to the second peak was found above B_p except in a close vicinity of T_c . We conclude that the role of even very fine secondary phase particles in formation of the second peak is indirect, a variation of the matrix properties on a microscopic scale being the principal pinning source responsible for fishtail effect.

Acknowledgements

M.J. greatly appreciates the JSPS fellowship covering his stay at Iwate University and the collaboration with ISTEK. Partial support was provided by the grant no. A1010919/99 of the Grant Agency of the ASCR, M. Muralidhar acknowledges support from NEDO fellowship.

References

- [1] M. Jirsa, M.R. Koblischka, T. Higuchi, M. Muralidhar, M. Murakami, Physica C 338 (2000) 235.
- [2] D. Dew-Hughes, Philos. Mag. 30 (1974) 293.

- [3] M. Muralidhar, M.R. Koblishka, M. Murakami, *Eur. Phys. J. (Appl. Phys.)* 7 (1999) 99.
- [4] H.P. Wiesinger, F.M. Sauerzopf, H.W. Weber, *Physica C* 203 (1992) 121.
- [5] M. Jirsa, M. Muralidhar, M. Murakami, K. Noto, T. Nishizaki, N. Kobayashi, *Supercond. Sci. Technol.* 14 (2001) 50–57.
- [6] M.R. Koblishka, M. Muralidhar, M. Murakami, in: T. Yamashita, K. Tanabe (Eds.), *Advances in Superconductivity XII*, Springer, Tokyo, 2000, p. 359.
- [7] T. Mochida, N. Chikumoto, M. Murakami, *Phys. Rev. B* 62 (2000) 1350.
- [8] G.K. Perkins, L.F. Cohen, A.A. Zhukov, A.D. Caplin, *Phys. Rev. B* 51 (1995) 8513.
- [9] G.K. Perkins, A.D. Caplin, *Phys. Rev. B* 54 (1996) 12551.
- [10] M. Jirsa, L. Püst, D. Dlouhý, M.R. Koblishka, *Phys. Rev. B* 55 (1997) 3276.
- [11] M. Jirsa, L. Püst, *Physica C* 291 (1997) 17.
- [12] M. Muralidhar, M.R. Koblishka, T. Saitoh, M. Murakami, *Supercond. Sci. Technol.* 11 (1998) 1349.